

# Thin current sheets as part of the substorm process

T. I. Pulkkinen, C. C. Goodrich, J. G. Lyon, and H. J. Singer

**Abstract:** This paper reviews properties of thin current sheets and their association with a variety of magnetospheric activations. It is demonstrated that thin current sheets are a major part of substorm growth phases as well as of sawtooth events and steady convection intervals. Observations, empirical models, and MHD simulations suggest that thin current sheets have thickness of the order of ion gyroradius, cross-tail width about 15–25  $R_E$  and along-tail dimension of about 20  $R_E$ . The current sheet inner edge is typically at or slightly tailward of geostationary orbit; during storms it can extend around the Earth in the duskward direction. As global simulations suggest that the magnetotail flow is diverted around the thin current sheet to the flanks in the inner part of the tail, the temporal scale associated with the current sheet intensification and thinning may play a role in determining the type of activity developing in the magnetotail.

*Key words:* Substorms, Thin current sheets, MHD simulations.

## 1. Introduction

Formation of an intense and thin current sheet in the inner part of the magnetotail is a well-documented feature of the substorm growth phase. This process is an indication of flux loading in the magnetotail as a consequence of enhanced dayside reconnection following southward turning of the interplanetary magnetic field (IMF) [1]. However, it has been shown that the thinning is stronger than that obtained by compression by the enhanced lobe pressure. Theoretically, it has been argued that thin current sheets are formed as a response to changing boundary conditions at the magnetopause [18].

It has been suggested that thin current sheets play an important role in the substorm onset process by thinning the tail sufficiently to demagnetize the ions and thereby destabilizing the ion tearing instability and initiating reconnection in the mid-magnetotail [3]. While the current sheet has been demonstrated to reach such small thickness values [14, 19, 17], the tearing instability growth conditions are still under debate [12].

During isolated substorms, thin current sheet formation is a slow process with gradual thinning over the duration of the growth phase (typically 30–60 min). At onset, this current is disrupted, which leads to rapid reconfiguration of the tail field to a more dipolar state. During the recovery phase, gradual tail current buildup brings the tail to its nominal state. On the other hand, the role of thin current sheets during storms, storm-time substorms, sawtooth events, or steady convection periods (SMC) has not been systematically examined.

We review properties of thin current sheets during a variety of activity conditions. The results are derived from observations, empirical models, and global magnetohydrodynamic (MHD) simulations. Section 2 briefly reviews the methodology while sections 3, 4, and 5 present results for isolated substorms, sawtooth events, and SMC periods, respectively.

Received 15 May 2006.

**T. I. Pulkkinen.** Los Alamos National Laboratory, Los Alamos, NM

**C. C. Goodrich.** Boston University, Center for Space Physics, Boston, MA

**J. G. Lyon.** Dartmouth College, Dept. of Physics and Astronomy, Hanover, NH

**H. J. Singer.** Space Environment Center, Boulder, CO

## 2. Methodology

Empirical magnetic field models [22, 23] give an average representation of the magnetospheric field configuration based on statistical fitting of parametrized current systems to a large number of spacecraft observations. While these models provide a good general understanding of the magnetic environment, they do not necessarily give an accurate representation of the field for individual events, especially during complex magnetic activity. However, these models have been used as starting points for event-specific models created by fitting the field model to data from individual substorms [14]. The fitting procedure includes current systems in the statistical model together with added current systems representing the (growth-phase-associated) thin current sheet at the tail center [14] and storm-time symmetric and partial ring currents in the inner magnetosphere [5]. The resulting time-evolving models have been shown to provide quite an accurate representation of magnetospheric magnetic field when sufficient data are available for the fitting procedure.

Global MHD simulations are presently the only means to model the large-scale dynamic evolution of the coupled solar wind – magnetosphere – ionosphere system in a self-consistent way. The Lyon-Fedder-Mobarry (LFM) global MHD simulation solves the ideal MHD equations in the solar wind and the magnetosphere, and is coupled to an electrostatic, height-integrated ionosphere via field-aligned currents at the inner boundary [4]. The simulation is driven by measured solar wind and IMF values at the external boundaries as well as the F10.7 flux that controls the level of ionization in the ionosphere. The spatial resolution in the code is variable, with highest resolution within the inner magnetosphere, plasma sheet, and boundaries where the gradients can be expected to be largest. Comparisons of simulation results with high-altitude satellite data as well as with ionospheric parameters show that these simulations can quite realistically represent a variety of dynamic conditions in the magnetotail [24].

## 3. Isolated substorm

During isolated substorms, when the tail is in a relatively low-energy state at the beginning of the growth phase, the formation of the thin current sheet is clearly seen as an enhancement

of  $B_X$  and a decrease in  $B_Z$  both in the inner and midtail. Figure 1 shows an example of a substorm during which the magnetotail field was monitored by GOES-8 and GOES-9 at geostationary orbit, Geotail in the plasma sheet, and Interball Tail probe in the tail lobe (all in GSM coordinates) [13]. As Geotail was relatively close to the current sheet center, it was possible to deduce that the current sheet became thinner than it would only following from compression caused by the lobe flux increase (which would be about a factor of 2 for a lobe flux increase from 20 to 30 nT). Thus, the thin current sheet was embedded within the (pre-existing) thicker plasma sheet.

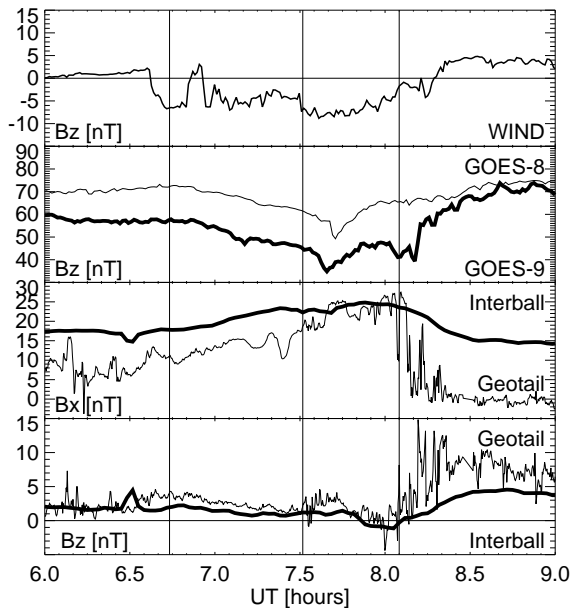


**Fig. 1.** Substorm on Dec 10, 1996: From top to bottom: IMF  $B_Z$  from Wind,  $B_Z$  from GOES-8 (thin line) and GOES-9 (thick line),  $B_X$  and  $B_Z$  from Geotail (thin line) and Interball (thick line). The vertical lines mark the beginning of substorm growth phase and two following onsets determined from the Geotail measurements and ground magnetic data, respectively [13].

Empirical magnetic field modeling for the growth phase of this substorm using methods developed in [14] show that a thin and intense current sheet was formed with its earthward edge slightly tailward of geostationary orbit. In the tailward and cross-tail directions, the current sheet extended at least to the satellite locations, but from this technique it is difficult to limit the extent of the current sheet. However, the model gave lower limits of  $-20R_E$  in the tailward and  $15R_E$  in the cross-tail direction [13].

The LFM simulation was run for this event at high resolution with smallest gridsize of  $0.3 R_E$ . Figure 2 shows a cut near the equatorial plane of the plasma sheet with the cross-tail current intensity color-coded and velocity vectors shown with white arrows. The thin current sheet in the simulation is the region of highest current density shown with the warmer colors, roughly extending from  $-8R_E$  to  $-20R_E$  along the tail and from  $-5R_E$  to  $5R_E$  in the cross-tail direction. The thin cur-

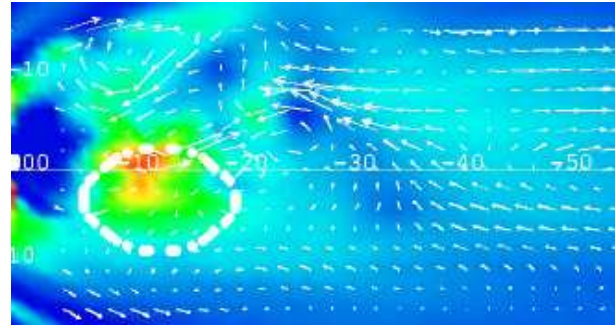


**Fig. 2.** Substorm on Dec 10, 1996: LFM simulation results at  $Z = \text{const}$  plane near the current sheet center. The color coding shows the cross-tail current intensity with warmer colors showing larger intensity. The arrows show the flow velocity and the dotted circle marks the thin current sheet location in the empirical magnetic field model (see text, after [13]).

rent sheet identified from the empirical magnetic field model described above is shown with the white dotted circle. In this case, the empirical model and the MHD simulation were in excellent agreement. Similar values obtained for other events suggest that a typical location of thin current sheets extends from slightly beyond geosynchronous orbit out to  $20\text{--}30 R_E$  in the tail, i.e., to the typical location of the near-Earth reconnection site [9].

#### 4. Sawtooth event

Sawtooth events are strong, quasiperiodic injections observed most clearly in geosynchronous orbit ion measurements [2, 7]. These events resemble large substorms in many ways, but have received special attention due to their large azimuthal extent and quasi-periodicity. Sawtooth events are almost always associated with magnetic storms during which the enhanced ring current allows for activity development close to the Earth.

Figure 3 shows a sample sawtooth event that occurred during a magnetic cloud passage. The main phase of the storm was driven by the sheath region of the cloud, while the cloud proper had  $B_Z$  northward at the leading edge and southward at the trailing edge [15]. The sawtooth event commenced as soon as the IMF turned southward within the cloud; during the following 10 hours, four clear sawtooth-like injections were recorded at multiple locations around the geostationary orbit.

During the sawtooth oscillations, two LANL geostationary satellites, LANL-97A and 1994-084 were passing through the evening-midnight sector magnetosphere. These satellites carry magnetospheric plasma analyzers (MPA) that measure electrons and protons in the energy range from below 1 keV up to 40 keV. The magnetic field inclination can be deduced from the electron or ion pitch-angle symmetry properties [21]. Both satellites recorded extremely strong stretching of the night and dusk sector field, with very low field inclination values even several hours away from midnight. Figure 3 shows the field inclination measurements together with the energetic electron data from the synchronous orbit particle analyzer (SOPA) on-board 1994-084.

The empirical magnetic field model for this event revealed a very strong modulation of the cross-tail current by the sawtooth

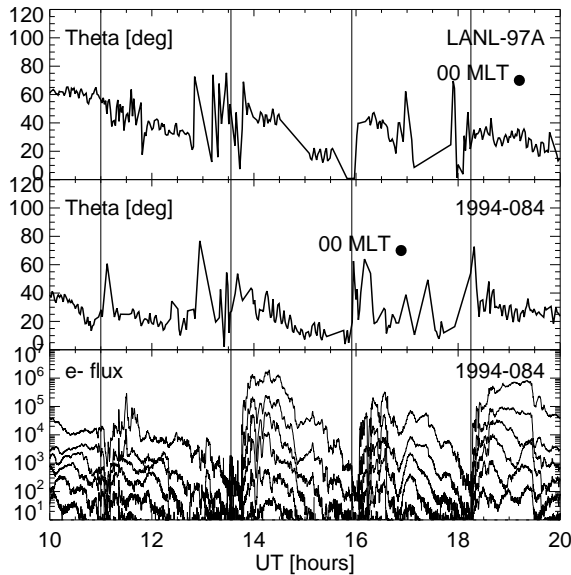


**Fig. 3.** Sawtooth event on Oct 22, 2001: Magnetic field inclination from geostationary satellites LANL-97A and 1994-084. Bottom panel shows electron flux in the energy range from 50 keV to 300 keV from s/c 1994-084 (after [15]).

injections. The current increased strongly between the sawteeth, while the injections were followed by abrupt decreases in the current intensity [15]. As shown in Figure 4, the event was characterized by a strongly asymmetric partial ring current in the dusk sector that varied in phase with the cross-tail current. The strong activity brought the thin current sheet inside geostationary orbit and drifting particles extended the current sheet to the dusk sector. The sawtooth injections periodically disrupted part of this current, but the field never fully dipolarized to values exceeding the quiet-time inclination value. This behavior is characteristic of sawtooth events, but is also often found during other stormtime activations [11].

Thus, in this case the activity was strong enough to bring the cross-tail current to the synchronous orbit, and the thin current sheet had a larger than typical cross-tail size extending around the Earth to the dusk sector. The sawtooth injections disrupted this current in a manner quite similar to current disruptions observed in association with substorm onsets.

## 5. Steady convection event

The steady convection event on Feb 3–4, 1998, was driven by an interplanetary magnetic cloud that had a steadily southward  $B_Z$ , a slowly rotating  $B_Y$ , and positive  $B_X$ . The solar wind velocity had a large component away from the Sun-Earth line, which led to rotation of the entire magnetotail in the direction of the solar wind flow. The  $V_Z$  component varied but reached values close to  $-100$  km/s, while  $V_Y$  rotated from about  $50$  km/s to  $-50$  km/s (Figure 5). The cloud caused only moderate activity with Kp between 2 and 4 during the event

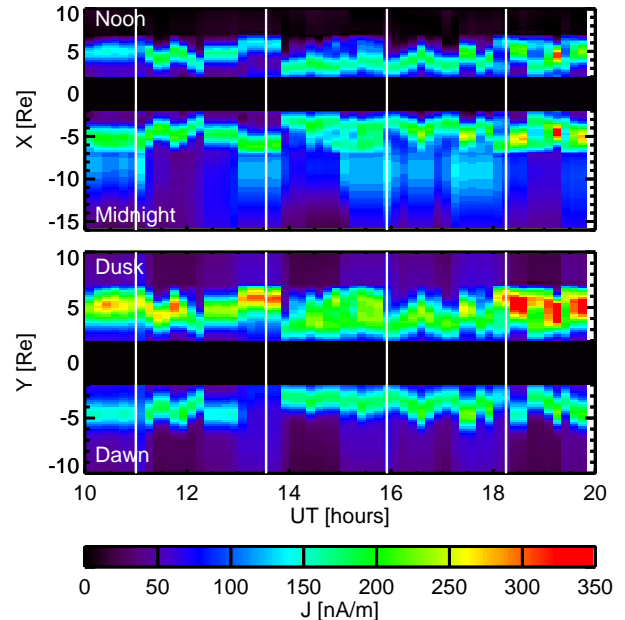


**Fig. 4.** Sawtooth event on Oct 22, 2001: Empirical magnetic field model results of  $Z$ -integrated current intensity through the noon-midnight (top panel) and dawn-dusk (bottom panel) meridians (after [15]).

and Dst minimum at about  $-40$  nT.

While the dayside geostationary field was close to quiet-time values as measured by GOES-8 and GOES-9, the nightside field inclination inferred from the MPA data from spacecraft 1994-084 and LANL-97A indicate that the inner tail field was stable and continuously more stretched than during quiet times. Geotail was at  $\sim X = -30R_E$  slightly below the GSM  $Z = 0$  plane. Immediately following the event onset, the magnetic field increased and temperature and density showed very small values (data not shown). These data indicate that Geotail moved to the northern tail lobe where it stayed throughout the SMC interval. Because the large solar wind velocity tilted the tail away from the Sun-Earth line, Figure 5 shows the Geotail magnetic field measurements rotated to a coordinate system aligned with the flow velocity vector. In this coordinate system it is clear that the magnetic field was very close to radial and that the field component normal to the current sheet at Geotail location was almost zero.

The LFM simulation was run for this event at a resolution which gives smallest cell size at the current sheet of about  $1R_E$ , which naturally limits the model capability to reproduce current sheet features below this scale. However, the simulation shows excellent agreement with both geosynchronous orbit and tail field measurements indicating that the large-scale properties of the current sheet are consistent with those observed. Figure 6 shows a comparison of both the geostationary orbit field inclination and Geotail (all in GSM coordinates) with the model results.

The LFM results show that immediately following the event onset, the tail organized into a very stable configuration where the plasma sheet was relatively thick, but had an embedded

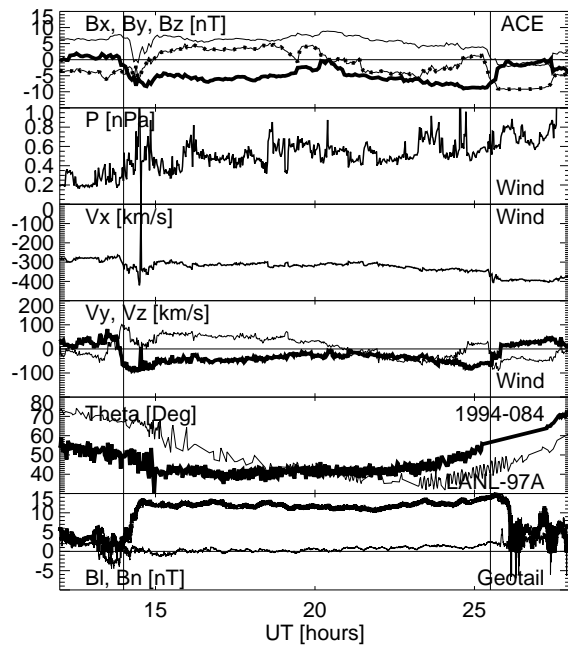


**Fig. 5.** SMC event on Feb 3–4, 1998: From top to bottom: IMF  $B_X$  (thin line),  $B_Y$  (dotted) and  $B_Z$  (Thick line) from ACE, propagated to subsolar point by 75 min. Solar wind dynamic pressure,  $V_X$ ,  $V_Y$  (thin line), and  $V_Z$  (thick line) from Wind, propagated to the subsolar point by 75 min. Geosynchronous orbit field inclination from LANL-97A (thin line) and from 1994-084 (thick line). Geotail magnetic field measurements rotated to coordinates along the solar wind flow velocity vector,  $B_{lobe}$  (thick line) and  $B_{normal}$  (thin line).

current sheet that had a scale size of about  $1R_E$ , i.e., thickness of the order of the grid spacing. The current sheet inside of  $X = -30R_E$  was remarkably stable throughout the event. There was a quasi-steady-state large-scale reconnection site at about  $X = -30R_E$  [6], but instead of disrupting the current sheet, flows from the reconnection region were diverted to the flanks around the thin current sheet. Thus, the persistent thin current sheet was a key factor in maintaining tail stability over the extended period of enhanced driving.

Figure 7 shows a side view and Figure 8 a top view of a rendering of  $B/|\nabla \times \mathbf{B}|$ , which is a proxy for the scale length in the direction perpendicular to the current sheet. As the rendering looks through all  $Y$  or  $Z$ -values, it is not sensitive to the correct choice of the cut-plane, but reflects the properties of the current sheet at all values perpendicular to the plane shown. The side view illustrates the steady thickness scale of the order of an Earth radius of the current sheet throughout the central part of the tail as well as the southward tilting of the current sheet in response to the nonradial component of the solar wind flow. The top view shows the flows originating from the reconnection region and how the flows are diverted around the current sheet without disrupting the current. It is clear that smaller-scale activity is created by the reconnection flows, but that the activity does not reach the inner part of the tail and does not cause global reconfigurations such as those observed during substorms.

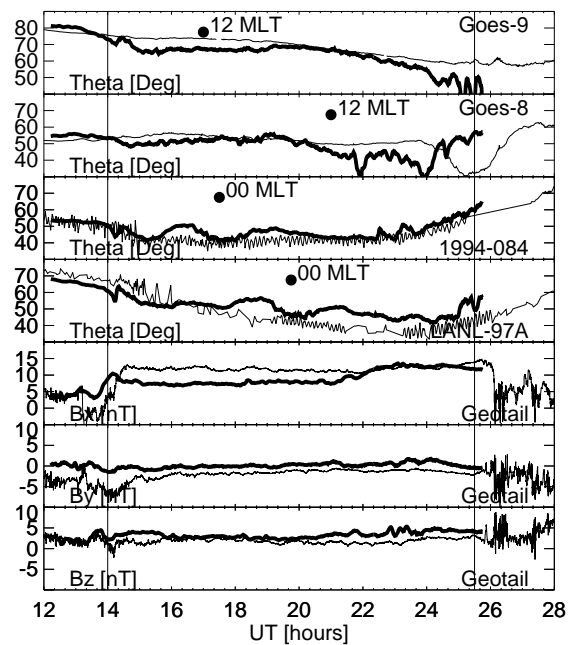


**Fig. 6.** SMC event on Feb 3–4, 1998: From top to bottom: Field inclination from GOES 9, GOES-8, 1994-084, and LANL-97A and 1984-084, and Geotail  $B_X$ ,  $B_Y$ , and  $B_Z$ . Data (in GSM coordinates) are shown with thin lines and LFM simulation results with thick lines.

## 6. Discussion

In response to solar wind driving, the magnetosphere can enter a variety of dynamic cycles to process the energy entering through enhanced dayside reconnection. In the large scale, tail reconnection in some form is required to maintain flux balance between the open tail lobes and the closed plasma sheet region. However, flow bursts, pseudobreakups, substorms, steady convection events, and sawtooth events can all accomplish the flux balance while their dynamics in the magnetosphere – ionosphere system is very different. Magnetic storms can host a variety of these activations in addition to a strong enhancement of the inner magnetosphere ring current, which allows activity to develop much closer to the Earth than during non-storm conditions.

Global MHD simulations are excellent tools to monitor the large-scale evolution of the tail plasma sheet during a variety of driving conditions. The LFM simulations consistently show that as the IMF turns southward, the inner part of the tail becomes thinner and the current intensity increases at the tail center in a region Earthward of about  $X = -20...-30R_E$ . The concentration of the current and changes in the inner part of the magnetosphere are easily explained by following Poynting flux flow lines from the solar wind to the magnetosphere [10]: Poynting flux ( $S = E \times B/\mu_0$ ) entering through the magnetopause into the tail lobe is directed toward the tail center, and as the field tilts northward closer to the current sheet, the Poynting flux is directed Earthward. Thus, it is natural that the largest changes are associated with the region where the dipole field still gives a contribution to the total field.

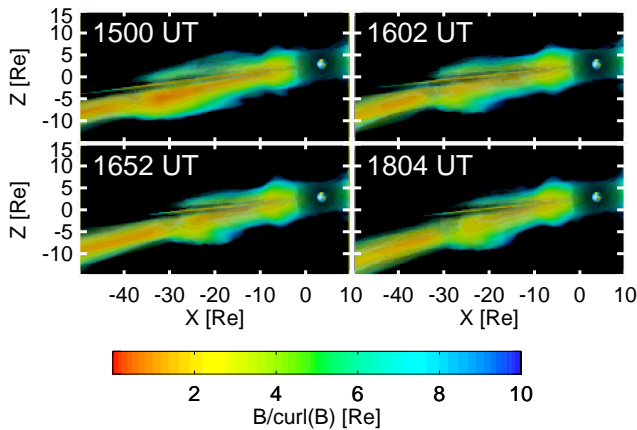


**Fig. 7.** SMC event on Feb 3–4, 1998: Side view of the current sheet at four time instants, at 1500, 1602, 1652, and 1804 UT. The color coding shows a perpendicular scale length ( $B/|\nabla \times \mathbf{B}|$ ) in units of  $R_E$ . The fine line across the current sheet is an artefact arising from the grid structure.

As the driving continues, reconnection starts near the tailward end of the current sheet and fast flows begin to enter the inner magnetosphere. In the LFM simulation, the dynamics and consequences of these flows are different for substorms, sawtooth events, and steady convection periods. During substorms, fast but relatively narrow flow channels are formed already during the growth phase (one example can be seen in Figure 2). These flow channels may disrupt part of the current sheet, but most of the time get diverted back tailward before affecting the current sheet very much [24]. At substorm onset, the flow channels merge to form a large-scale reconnection region and fast flows that disrupt the cross-tail current in the inner tail. Steady convection periods have a relatively large-scale reconnection region from early on, but the flows are mostly diverted toward the flanks leaving the current sheet intact (see Figures 7 and 8). The flows fed by a large-scale reconnection region associated with sawtooth events are much more complicated with flow channels occasionally gaining access to the inner parts of the tail partially disrupting the inner tail current [6]. The simulations seem to indicate that the type of magnetospheric activity is determined by the interplay of the reconnection flows and the thin current sheet in the inner tail.

Observations and empirical models suggest that the thin current sheet has a scale thickness of a fraction of  $R_E$ , comparable to the local thermal ion gyroradius. The MHD simulations tend to give current sheet thicknesses of the order of the simulation gridsize; increasing resolution leads to thinner current sheets. As the current sheet reaches such small thickness, the ions within the current sheet become non-magnetized and the electron and ion motions are decoupled. While the reconnection region is typically found to be around  $25 - 30R_E$  distance, the nonadiabatic regime can extend to  $8 - 10R_E$  or during stronger activity even close to geostationary orbit. It thus seems that rather than triggering reconnection onset, the role of the nonadiabatic motion is to allow the flows initiated by bursts of reconnection to enter the inner parts of the tail and disrupt the intense current. This still leaves open the question why or

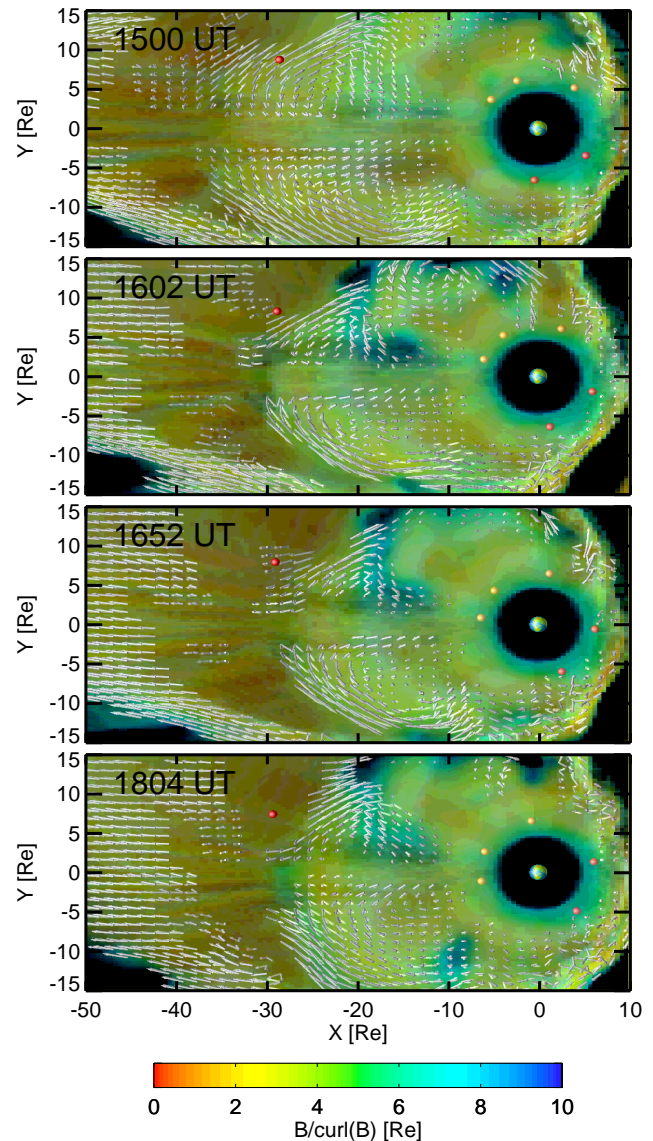


**Fig. 8.** SMC event on Feb 3–4, 1998: Top view of the current sheet at four time instants, at 1500, 1602, 1651, 1804 UT. The color coding shows a perpendicular scale length ( $B/|\nabla \times \mathbf{B}|$ ) in units of  $R_E$  and the flow velocity is shown by arrows.

how reconnection is initiated in the midtail; in the MHD simulations tail reconnection seems to be quite directly driven by the external conditions and the amount of energy entering the magnetosphere [8, 16].

An interesting feature observed during storms is the extension of the thin current sheet duskward (or sometimes dawnward) such that the geostationary field can become highly stretched even several hours away from midnight. Especially, during sawtooth events, the combination of the partial ring current and cross-tail current is very strong such that even the intense sawtooth injections can only partially disrupt this current (see Figures 3 and 4). Such a current configuration also leads to the geostationary orbit being in the region of open drift paths,

which limits the number of particles that can obtain trapped orbits and leads to the typically relatively constant values of the Dst index throughout sawtooth events [15]. However, despite the different geometry of the current sheet, the dynamics seems to be quite similar to those limited to the tail region.

In summary, thin current sheets play a major role in controlling the magnetospheric dynamics. Flows entering the inner part of the tail are diverted by the intense current; this occurs during substorm growth phases as well as during SMCs and between sawtooth injections. Global reconfigurations such as substorm onsets or sawtooth injections occur when the flows finally enter the current sheet leading to its disruption and consequent field dipolarization. Future work is needed to address how much the current sheet dynamics is controlled by internal magnetospheric (or ionospheric) processes and to which extent the dynamics is driven by the driving solar wind and IMF characteristics.

### Acknowledgements

Dr. K. Ogilvie (PI for Wind SWE) and Dr. C. Smith (PI for ACE MFI) are acknowledged for providing the solar wind observations obtained through the CDAWeb data facility operated and maintained by the NSSDC. We thank T. Nagai and the DARTS system at ISAS for making the Geotail LEP and MFI data available.

### References

- Baker, D. N., T. I. Pulkkinen, V. Angelopoulos, W. Baumjohann, and R. L. McPherron, The neutral line model of substorms: Past results and present view, *J. Geophys. Res.*, *101*, 12,975, 1996.
- Belian, R. D., T. E. Cayton, and G. D. Reeves, Quasi-periodic global substorm-generated variations observed at geosynchronous orbit, in: *Space plasmas: Coupling between small and medium scale processes*, Geophys. Monogr., 86, AGU, Washington DC 20009, p. 143, 1995.
- Büchner, J., and L. M. Zelenyi, Chaotization of the electron motion as the cause of an internal magnetotail instability and substorm onset, *J. Geophys. Res.*, *92*, 13456, 1987.
- Fedder, J. A., S. P. Slinker, J. G. Lyon, and R. D. Elphinstone, Global numerical simulation of the growth phase and expansion onset for a substorm observed by Viking, *J. Geophys. Res.*, *100*, 19,083, 1995.
- Ganushkina, N. Yu., T. I. Pulkkinen, M. V. Kubyshkina, H. J. Singer, and C. T. Russell, Long-term evolution of magnetospheric current systems during storm periods, *Ann. Geophys.*, *22*, 1317, 2004.
- Goodrich, C. C., et al., this issue.
- Henderson, M. G., G. D. Reeves, R. Skoug, M. F. Thomsen, M. H. Denton, S. B. Mende, T. J. Immel, P. C. Brandt, and H. J. Singer, Magnetospheric and auroral activity during the 18 April 2002 sawtooth event, *J. Geophys. Res.*, *111*, A01S90, doi:10.1029/2005JA011111, 2006.
- T. V. Laitinen, T. I. Pulkkinen, M. Palmroth, P. Janhunen, and H. E. J. Koskinen, The magnetotail reconnection region in a global MHD simulation, *Ann. Geophys.*, *23*, 3753, 2005.
- Nagai, T., M. Fujimoto, Y. Saito, S. Machida, T. Terasawa, R. Nakamura, T. Yamamoto, T. Mukai, A. Nishida, and S. Kokubun, Structure and dynamics of magnetic reconnection for substorm onsets with Geotail observations, *J. Geophys. Res.*, *103*, 4419, 1998.
- Papadopoulos, K., C. Goodrich, M. Wiltberger, R. Lopez, and J. G. Lyon, The physics of substorms as revealed by the ISTP, *Phys. Chem. Earth (c)*, *24*, 189, 1999.
- Partamies, N., T. I. Pulkkinen, E. I. Tanskanen, G. D. Reeves, E. F. Donovan, H. J. Singer, J. A. Slavin, R. L. McPherron, and M. Henderson, Strong stretching in dusk sector: storm-time substorms and sawtooth events compared, *this issue*, 2006.
- Pellat, R., F. Coroniti, and P. L. Pritchett, Does iontearing exist? *Geophys. Res. Lett.*, *18*, 143, 1991.
- Pulkkinen, T. I., and M. Wiltberger, Thin Current Sheet Evolution as seen in Observations, Empirical Models and MHD Simulations, *Geophys. Res. Lett.*, *27*, 1363, 2000.
- Pulkkinen, T. I., D. N. Baker, R. J. Pellinen, J. Büchner, H. E. J. Koskinen, R. E. Lopez, R. L. Dyson, and L. A. Frank, Particle scattering and current sheet stability in the geomagnetic tail during the substorm growth phase, *J. Geophys. Res.*, *97*, 19,283, 1992.
- Pulkkinen, T. I., N. Yu. Ganushkina, E. I. Tanskanen, M. Kubyshkina, G. D. Reeves, C. T. Russell, H. J. Singer, J. A. Slavin, Magnetospheric current systems during stormtime sawtooth events, *J. Geophys. Res.*, submitted, 2006.
- Pulkkinen, T. I., M. Palmroth, E. I. Tanskanen, P. Janhunen, H. E. J. Koskinen, and T. V. Laitinen, New interpretation of magnetospheric energy circulation, *Geophys. Res. Lett.*, *33*, L071101, doi:10.1029/2005GL025457, 2006.
- Runov, A., R. Nakamura, W. Baumjohann, R. A. Treumann, T. L. Zhang, M. Wolwerk, Z. Voros, A. Balogh, K.-H. Glassmeier, B. Klecker, H. Reme, and L. Kistler, Current sheet structure near magnetic X-line observed by Cluster, *Geophys. Res. Lett.*, *30*, 11, 1579, doi: 10.1029/2002GL016730, 2003.
- Schindler, K., and J. Birn, On the cause of thin current sheets in the near-Earth magnetotail and their possible significance for magnetospheric substorms, *J. Geophys. Res.*, *98*, 15477, 1993.
- Sergeev, V. A., D. G. Mitchell, C. T. Russell, D. J. Williams, Structure of the tail plasma/current sheet at 11 Re and its changes in the course of a substorm, *J. Geophys. Res.*, *98*, 17345, 1993.
- Thomsen, M. F., S. J. Bame, D. J. McComas, M. B. Moldwin, K. R. Moore, The magnetospheric lobe at geosynchronous orbit, *J. Geophys. Res.*, *99*, 17,283, 1994.
- Thomsen, M. F., D. J. McComas, G. D. Reeves, and L. A. Weiss, An observational test of the Tsyganenko (T89a) model of the magnetospheric field, *J. Geophys. Res.*, *101*, 24827, 1996.
- Tsyganenko, N. A., Magnetospheric magnetic field model with a warped tail current sheet, *Planet. Space Sci.*, *37*, 5, 1989.
- Tsyganenko, N. A., Modeling the Earth's magnetospheric magnetic field confined within a realistic magnetopause, *J. Geophys. Res.*, *100*, 5599, 1995.
- Wiltberger, M., T. I. Pulkkinen, J. G. Lyon, and C. C. Goodrich, MHD simulation of the magnetotail during the December 10, 1996 substorm, *J. Geophys. Res.*, *105*, 27649, 2000.